TISSUE ENGINEERING: Part A
Volume 20, Numbers 3 and 4, 2014

DOI: 10.1089/ten.tea.2013.0092

Enhanced Femoral Nerve Regeneration After Tubulization with a Tyrosine-Derived Polycarbonate Terpolymer: Effects of Protein Adsorption and Independence of Conduit Porosity

Mindy Ezra, PhD,[1,2] Jared Bushman, PhD,[1] David Shreiber, PhD,[2]
Melitta Schachner, PhD,[3] and Joachim Kohn, PhD[1,4]

Following complete nerve transection, entubulation of the nerve stumps helps guide axons to reconnect distally. In this study, a biodegradable and noncytotoxic tyrosine-derived polycarbonate terpolymer composed of 89.5 mol% desaminotyrosyl tyrosine ethyl ester (DTE), 10 mol% desaminotyrosyl tyrosine (DT), and 0.5 mol% poly(ethylene glycol) (PEG, molecular weight [Mw] = 1 kDa) [designated as E10-0.5(1K)] was used to fabricate conduits for peripheral nerve regeneration. These conduits were evaluated against commercially available nonporous polyethylene (PE) tubes. The two materials are characterized *in vitro* for differences in surface properties, and the conduits are then evaluated *in vivo* in a critical-sized nerve defect in the mouse femoral nerve model. Conduits were fabricated from E10-0.5(1K) in both porous [P-E10-0.5(1K)] and nonporous [NP-E10-0.5(1K)] configurations. The results illustrate that adsorption of laminin, fibronectin, and collagen type I was enhanced on E10-0.5(1K) compared to PE. In addition, *in vivo* the E10-0.5(1K) conduits improved functional recovery over PE conduits, producing regenerated nerves with a fivefold increase in the number of axons, and an eightfold increase in the percentage of myelinated axons. These increases were observed for both P-E10-0.5(1K) and NP-E10-0.5(1K) after 15 weeks. When conduits were removed at 7 or 14 days following implantation, an increase in Schwann cell proteins and fibrin matrix formation was observed in E10-0.5(1K) conduits over PE conduits. These results indicate that E10-0.5(1K) is a pro-regenerative material for peripheral nerves and that the porosity of P-E10-0.5(1K) conduits was inconsequential in this model of nerve injury.

Introduction

Peripheral nerve injuries present a serious medical concern, constituting ~2.8% of all trauma cases in the United States, and ~100,000 neurosurgical procedures in the United States and Europe annually.[1,2] Although peripheral nerves are able to regenerate, their regeneration often results in poor functional recovery. As axons extend across large gaps slowly, they often make random reconnections with axonal targets and do not reach the distal stump until long after denervation has already occurred.[3] This poor recovery leads to inadequate muscle contraction and coordination, poor reflexes, allodynia, and an overall lower quality of life.[4–6]

Methods of repair for peripheral nerve defects depend upon the severity of the injury. When the defect is small enough, nerve stumps can be directly sutured together, end-to-end.[7] However, when the defect is too extensive, grafts of sensory nerves, decellularized nerves, or synthetic conduits are sutured to the nerve stumps to act as a guide and protective space for the regenerating nerve.[8] Many naturally existing conduits can be used to bridge nerve gaps, including the vein, artery, muscle, or nerve segments.[9] Autologous nerves are preferred, yet limited availability of donor nerves, donor-site morbidity, and differences in the structure and size of the nerve are thought to limit recovery.[10,11] Complete recovery of motor and sensory nerve functions following an autograft procedure is still less than 50% of treatment cases, indicating the much needed necessity for improvement.[12]

Synthetic conduits are commonly used as an alternative to autografts for nerve regeneration, as there is no limitation on their supply, their chemical structure can be altered to adjust

[1]New Jersey Center for Biomaterials, Rutgers, The State University of New Jersey, Piscataway, New Jersey.
[2]Department of Biomedical Engineering, Rutgers, The State University of New Jersey, Piscataway, New Jersey.
[3]W.M. Keck Center for Collaborative Neuroscience, Rutgers, The State University of New Jersey, Piscataway, New Jersey.
[4]Department of Chemistry and Chemical Biology, Rutgers, The State University of New Jersey, Piscataway, New Jersey.

their properties, and they can be fabricated into designs with various dimensions to fit different size defects.[10,11] Nondegradable materials such as silicone have been fabricated into conduits and used for entubulation as they are inert, readily available, and able to facilitate repair of transected nerve gaps up to 3 cm in length.[13] Nondegradable polyethylene (PE) has shown similar capabilities, but thus far only in animal models.[14–16] Whereas these conduits have provided an important benchmark for nerve regeneration, their inability to degrade can result in chronic host tissue response and/or nerve compression months after implantation, deterring regeneration.[17–19]

To avoid these issues, biodegradable materials have been developed and utilized for the fabrication of nerve conduits. Studies from over the past 20 years have resulted in the approval by the U.S. Food and Drug Administration (FDA) of several biodegradable nerve conduits.[20] However, when these conduits are used empty in experimental and clinical studies, to treat injuries greater than the critical size,[21–23] nerve regeneration and functional recovery are significantly impaired as compared to autografts.[11,24–27] Ongoing issues, such as swelling that can occlude the inner lumen, inappropriate degradation rates, and cytotoxic degradation products, are believed to be associated with inhibiting regeneration.[2,9,28–30]

To meet the ongoing need for an optimal material for nerve conduits, we are exploring the library of tyrosine-derived polycarbonates. Tyrosine-derived polycarbonates are a combinatorially designed library of over 10,000 distinct polymer compositions. Within this library, specific polymer compositions have been discovered that offer optimum properties for the construction of coronary stents[31] and bone regeneration.[32] In general, these polymers cover a wide range of degradation and resorption rates,[33] a broad range of mechanical properties,[34] and exhibit long-term compatibility with the surrounding tissue.[35]

In this study, a specific tyrosine-derived polycarbonate composition (89.5 mol% desaminotyrosyl tyrosine ethyl ester [DTE], 10 mol% desaminotyrosyl tyrosine [DT], and 0.5 mol% of poly(ethylene glycol) [PEG] with Mw of 1 kDa) was evaluated for its potential to enhance nerve regeneration *in vitro* and *in vivo*. For brevity, this polymer is designated as E10-0.5(1K). The degradation time of this polymer is such that no significant degradation occurs during the timeline of the experiments outlined below. Therefore, any concerns regarding degradation are not confounding the results of the study. *In vitro* studies on two-dimensional (2D) substrates indicated that protein attachment and neurite outgrowth are significantly enhanced on E10-0.5(1K) as compared to PE. For an *in vivo* evaluation of nerve conduits fabricated from E10-0.5(1K), the mouse femoral nerve model, first introduced by Brushart,[36–38] was employed. This model is well-characterized and allows for both morphological and functional measures of recovery.[39–42] The femoral nerve is the sole innervating nerve to the quadriceps muscle. Loss of innervation to this muscle results in reliable and readily quantifiable deficiencies in the function of the affected limb that correspond to the histology of the regenerated nerve.[15,39,43] A critical size gap (5.4 ± 1.0 mm in a mouse) in the femoral nerve was used as the nerve injury.[21,44] Although other mouse nerve models have employed an autograft as a method of repair and compared it to a nondegradable silicone nerve conduit,[45] the use of a mouse femoral nerve autograft has not been performed to date. NP-PE conduits are commonly used in the mouse femoral nerve model[15,40] and were therefore chosen as a comparative treatment method to the use of E10-0.5(1K) conduits in this study. *In vivo* experiments found that both porous [P-E10-0.5(1K)] and nonporous [NP-E10-0.5(1K)] conduits supported significantly greater nerve regeneration and functional recovery than nonporous PE (NP-PE) conduits. Evaluation of recovery at early time points suggested that this enhancement is correlated with greater Schwann cell presence and a more rapid formation of the fibrin matrix, which are both key early features of peripheral nerve regeneration.

Materials and Methods

Conduit fabrication

E10-0.5(1K) (Fig. 1), synthesized utilizing previously published procedures,[46] was used in this study. Briefly, hollow conduits with an inner diameter of 580 μm were fabricated using a dip-coating (KSV dip-coater; KSV Instruments, Inc.) technique in which a Teflon-coated mandrel was dipped at a constant rate (40 mm/min) into a polymer solution. For nonporous conduits, a solution containing 900 mg of polymer in 3 mL of methylene chloride was used. For porous conduits, a solution of 450 mg of sucrose crystals, sieved to 25–45 μm, and 450 mg of polymer dissolved in 3 mL of methylene chloride was used. Following dip coating, the mandrels were dried in vacuum overnight, and conduits were pulled off and cut to 5 mm length for *in vivo* evaluation. For porous conduits, the sucrose was leached out in water to create a porous structure. Commercially available PE tubes were also used as nerve conduits (5 mm length, 0.58 mm inner diameter; Becton Dickinson).

In vitro *evaluations*

In vitro assessment of conduit material with spinal cord neurons and Schwann cells. The effect of E10-0.5(1K) and PE on neurite outgrowth and Schwann cell attachment and extension was determined using glass coverslips spin coated with E10-0.5(1K) (2.5% w/v solution in tetrahydrofuran) or coated with a thin self-adhering film of PE (VWR).

To facilitate cell survival and outgrowth, coverslips were coated with 200 μg/mL of poly-L-lysine (PLL; Sigma) followed by 20 μg/mL of laminin (Invitrogen). Embryonic spinal cord neurons were isolated and purified for a motor rich population. Schwann cells were isolated and purified from

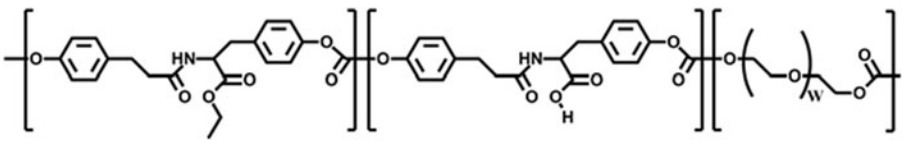

FIG. 1. Chemical structure of E10-0.5(1K) consisting of desaminotyrosyl tyrosine ethyl ester (DTE), desaminotyrosyl tyrosine (DT), and poly(ethylene glycol) (PEG).

the sciatic nerves of P2 neonates according to published protocols,[47] yielding cultures with >95% of cells staining positive for S100β. Cells were seeded onto coverslips (1.5×10^4 cells/coverslip) and maintained for 48 h at 37°C with 5% CO_2. Neurites and the process outgrowth of neurons and Schwann cells were evaluated using the β-tubulin antibody (Covance; 1:500) and S100β (Abcam; 1:500), respectively, with both cell types visualized using the Alexa Fluor 488 secondary antibody (Invitrogen). Nuclear staining was performed with Hoechst 33258 stain (AnaSpec, Inc.). The length of total neurites/processes per cell was measured using ImageJ (NIH). For each coverslip, 10 randomly chosen representative images were analyzed in a double-blind manner and neurites were binned based on their length.

Protein adsorption assay. The relative amounts of protein adsorption for three extracellular matrix (ECM) molecules (laminin [Invitrogen], fibronectin [Invitrogen], and collagen type I [Advanced Biomatrix]) on E10-0.5(1K) and PE films were evaluated. E10-0.5(1K) films prepared by compression molding and PE films (VWR) were fit into a 96-well plate. A 70 μL solution of each protein (20 μg/mL in ddH_2O) was added to each well and allowed to adhere to the films at 37°C for 48 h. After the supernatant was removed, each well was rinsed thoroughly and blocked with media containing fetal calf serum. After rinsing, the primary antibodies against each protein were added for 1 h at room temperature (Millipore; 1:100). The entire rinsing process was repeated, and a secondary horseradish peroxidase (HRP)-conjugated antibody (Millipore; 1:200 dilution) was added for 1 h at room temperature. The rinsing process was repeated once more, and Luminol (Invitrogen) was added to each well. After 5 min, the luminescence from each well was read using a Tecan plate reader with an integration time of 1000 ms and a settle time of 500 ms. Protein amounts were normalized to the control surface, tissue culture polystyrene.

In vivo *evaluation*

Surgical methods and animal groups. All experiments were conducted in accordance with the Institutional Animal Care and Use Committee (IACUC). Female C57BL/6J mice (age 3 months) were anesthetized by intraperitoneal injection of a ketamine (80 mg/kg) and xylazine (12 mg/mg) mixture. The left femoral nerve was surgically exposed, and a nerve transection was performed at a distance ~3 mm proximal to the bifurcation of the nerve. The cut ends of the nerve were inserted into the saline-filled nerve conduit and fixed on each end with a 10-0 nylon suture (Ethicon), so that a 5 mm gap was present between the proximal and distal stump. The incised skin was closed with wound clips, which were removed 2 weeks post-surgery. Three animal groups (eight animals each) receiving the three conduit types were compared over a 15-week time period, including P-E10-0.5(1K), NP-E10-0.5(1K), and NP-PE.

Motor function recovery. Functional recovery was assessed using a single-frame motion analysis approach (SFMA).[40] Animals were trained to perform a beam walking test before implantation of the conduit. Following surgery, this test was performed weekly until the endpoint of the experiment. Rear view videos of the mice walking were collected using a high-speed camera (A602fc; Basler). The movements of the hind legs during the normal gait cycle were analyzed from individual video frames using SimiMotion (SIMI Reality Motion Systems). The foot base angle (FBA)[40] was measured to evaluate the function of the quadriceps muscle. Additionally, the protraction limb ratio (PLR)[40] was measured, while the mouse performed a voluntary movement during a pencil grip test.

A recovery index (RI) was calculated for each animal for both the FBA and the PLR to provide a relative measure of functional recovery. The RI was calculated as a percentage using the following formula:

$$RI = \left[\frac{(X_{week\ y} - X_{week\ 1})}{(X_{week\ 0} - X_{week\ 1}}\right] \times 100,$$

where $X_{week\ 0}$, $X_{week\ 1}$, and $X_{week\ y}$ are intact values at week 0 (either FBA or PLR), values measured at week 1 after injury, and at week y (where y is the endpoint of the study, week 15), respectively.[40] An RI value of 100 indicates complete recovery of the femoral nerve.

Histomorphometric analysis of explanted nerve. Following perfusion with 4% paraformaldehyde at 16 weeks, femoral nerves were dissected from animals and morphometric analysis was performed according to the standard protocol.[48] The total number of myelinated axons per nerve cross section, raw tissue area, cross-sectional area of the regenerating cable, and the % nerve regeneration were measured with ImageJ. Axonal (inside the myelin sheath) and nerve fiber (including the myelin sheath) diameters were measured in a random sample from each section.

Western blot analysis of nerve exudates at 1 week *in vivo*. To evaluate the presence of Schwann cells within nerve conduits, western blot analysis of Schwann cell markers was performed on nerve exudates.[49] Conduits ($n=3$) were implanted into the mouse femoral nerve for 1 week after which animals were sacrificed and nerve exudates within the conduits were removed and run on an SDS-PAGE gel (Invitrogen) and transferred to PVDF membranes (Biorad). Membranes were blocked and probed with antibodies against S100β (1:1000), glial fibrillary acidic protein (GFAP, 1:50,000), GAPDH (1:1000), and β-actin (1:5000) (Abcam) and detected through HPR luminescence of secondary antibodies.[50] Densitometric analysis was performed to quantify band density of GFAP, S100β, and actin from the western blot using ImageJ (NIH). Amounts were normalized based on actin loading control.

Morphological analysis of fibrin matrix formation. Animals ($n=3$ per condition) were sacrificed at 2 weeks post-implantation to visualize the presence of fibrin strands. Nerve explants were postfixed in osmium tetroxide and embedded in resin according to the standard protocol. Longitudinal 1-μm-thick sections of the nerve were cut and stained with 1% toluidine blue/1% borax in distilled water. Conventional light microscopy was used to visualize the presence and orientation of the fibrin matrix.[51]

Statistical analysis. The study was designed to allow comparison of the effects of polymers E10-0.5(1K) and PE in

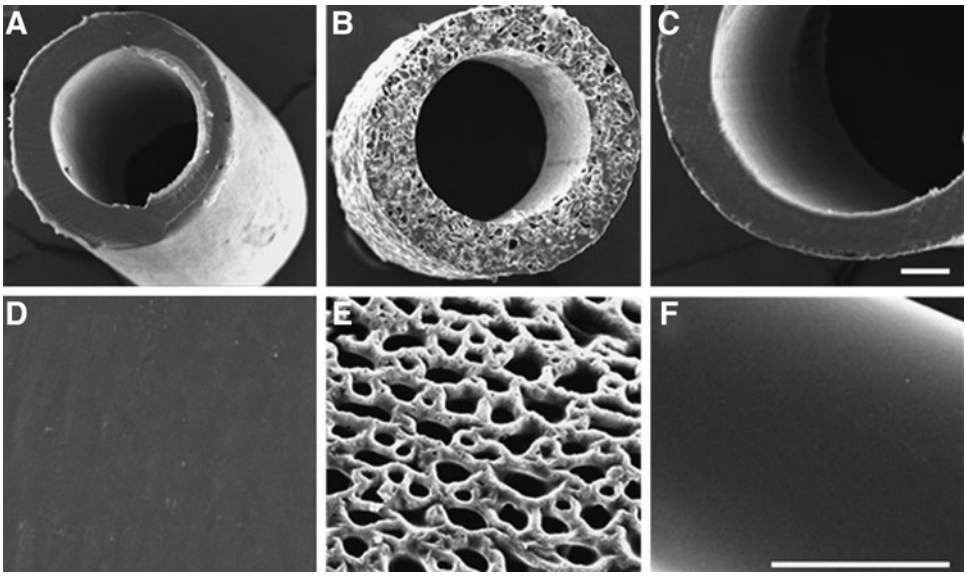

FIG. 2. Scanning electron microscope (SEM) images of conduits evaluated in this study. Cross sections of a **(A, D)** nonporous polyethylene (NP-PE) conduit, **(B, E)** porous E10-0.5(1K) [P-E10-0.5(1K)] conduit, and a **(C, F)** nonporous E10-0.5(1K) [NP-E10-0.5(1K)] conduit, respectively. Scale bar in each row: 100 μm.

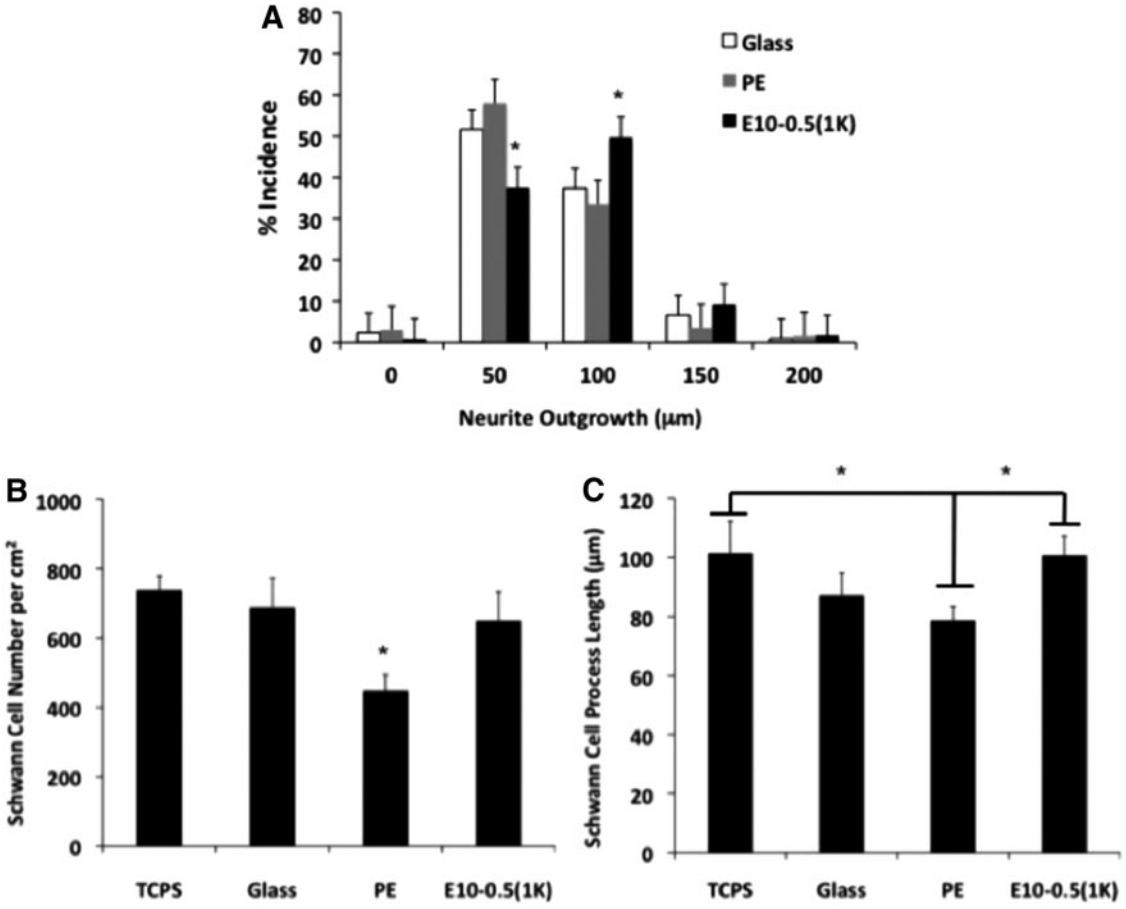

FIG. 3. *In vitro* evaluation of neurite outgrowth and Schwann cell proliferation and extension on two-dimensional (2D) films of E10-0.5(1K) and PE in comparison with control substrates, tissue culture polystyrene (TCPS), and glass. **(A)** Neurite outgrowth distribution of rat spinal cord motor neurons on polymer-coated glass coverslips precoated with poly-L-lysine (PLL) and laminin. Neurites were binned based on their length. Bar height shift to right indicates longer neurite extensions on E10-0.5(1K)-coated coverslips as compared to PE and glass coverslips. Significantly, more neurite extensions reached 100 μm on E10-0.5(1K)-coated coverslips as compared to neurite extensions on PE and glass coverslips. **(B)** Schwann cell density on polymer-coated glass coverslips precoated with PLL. Significantly less Schwann cells attached to PE substrates as compared to TCPS, glass, and E10-0.5(1K) at 24 h. **(C)** Schwann cell extension length (μm) on polymer-coated glass coverslips precoated with PLL. Schwann cells exhibited greater extension on TCPS and E10-0.5(1K) substrates as compared to PE at 24 h. (*$p < 0.05$, one-way analysis of variance with Tukey's *post hoc* test).

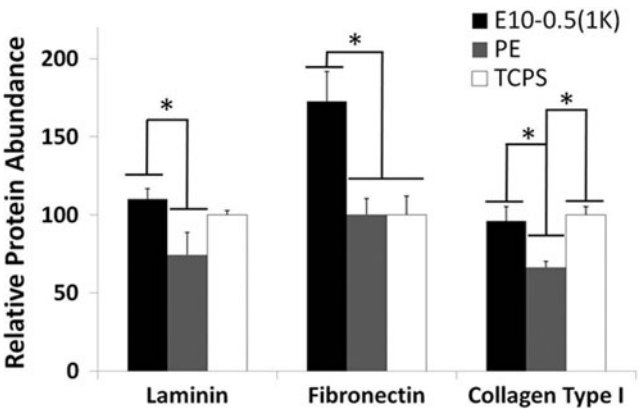

FIG. 4. Relative adsorption of neurosupportive extracellular matrix (ECM) proteins (laminin, fibronectin, and collagen type I) on 2D films of E10-0.5(1K) and PE in comparison with a control substrate, TCPS. (*$p < 0.05$, one-way analysis of variance with Tukey's *post hoc* test).

both a 2D and conduit fashion on nerve regeneration. Variance analysis using a one-way analysis of variance was used followed by *post hoc* planned comparisons with the Tukey's test. Differences were considered significant at $p < 0.05$.

Results

In vitro *characterization*

Both PE and E10-0.5(1K) nonporous conduits had a similar appearance based on SEM micrographs (Fig. 2A, D, C, F). The porous E10-0.5(1K) conduits had an interconnected pore structure, and the degree of porosity and mean pore size of the conduits were 55.2% ± 1.2% and 35.7 ± 9.0 μm, respectively (Fig. 2B, E). The conduits fabricated from E10-0.5(1K) are opaque, nonflexible (at the 5 mm lengths), have an internal diameter of 580 μm and an external diameter of 680 μm. All conduits remained intact throughout the study.

Material and cell studies revealed disparate properties among the conduit types. The response of motor neurons to the different materials was assessed on E10-0.5(1K) and PE 2D films coated with PLL and laminin. Longer axons were observed on E10-0.5(1K) when compared to PE (Fig. 3), as indicated by the peak shift of E10-0.5(1K) to the right of the PE and control substrate peaks. An assessment of Schwann cell attachment and extension of processes on the differing substrates revealed that E10-0.5(1K) similarly promoted these aspects as compared to PE (Fig. 3B, C). The adsorption of proteins essential to nerve regeneration to the different materials was also significantly different (Fig. 4). The amounts of three ECM proteins adsorbing to E10-0.5(1K) were significantly greater as compared to PE films.

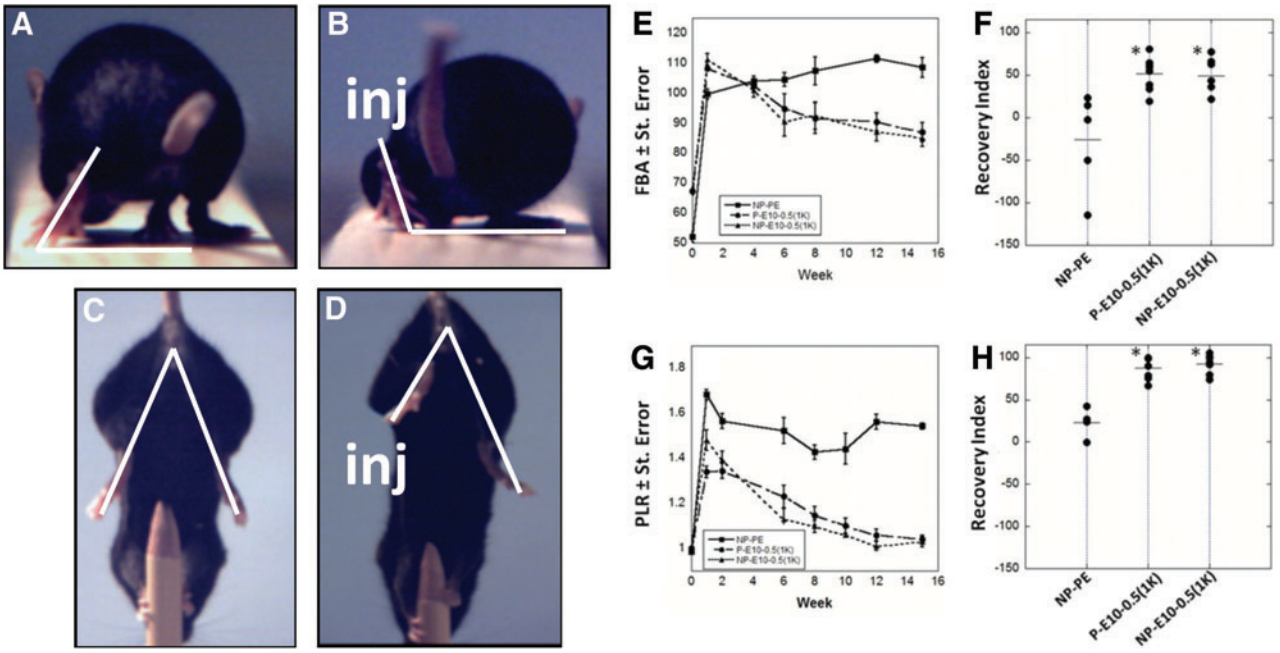

FIG. 5. Video frames showing the functional measurements performed on mice following implantation of the conduit and metrics of functional recovery promoted by E10-0.5(1K) and NP-PE conduits *in vivo*. Frames A and C represent pre-injury measurements and frames B and D represent post-injury (inj) measurements. The white lines drawn in the video frames show the foot base angle (FBA) **(A, B)**, and the limb lengths used for calculation of the protraction limb ratio (PLR) **(C, D) (A)** FBA of mice pre-injury averages 50–70°. **(B)** FBA of mice 1 week post-injury averages 90–110°. Functional recovery is denoted by a reduction in this degree angle. **(C)** The pencil grip test measures the PLR on a mouse pre-injury, where both limbs are similarly extended, giving a ratio of 1. **(D)** PLR on a mouse 1 week post-injury shows the disparity in limb protraction due to injury, resulting in a PLR > 1. **(E)** FBA for a 15-week period following surgical insertion of nonporous PE conduits (NP-PE), porous E10-0.5(1K) conduits [P-E10-0.5(1K)], and nonporous E10-0.5(1K) conduits [NP-E10-0.5(1K)] pre-filled with saline. **(F)** Recovery index for FBA at week 15. Each dot represents one animal. **(G)** PLR for all conditions. **(H)** Recovery Index for PLR at week 15. (*$p < 0.001$, one-way analysis of variance with Tukey's *post hoc* test). Color images available online at www.liebertpub.com/tea

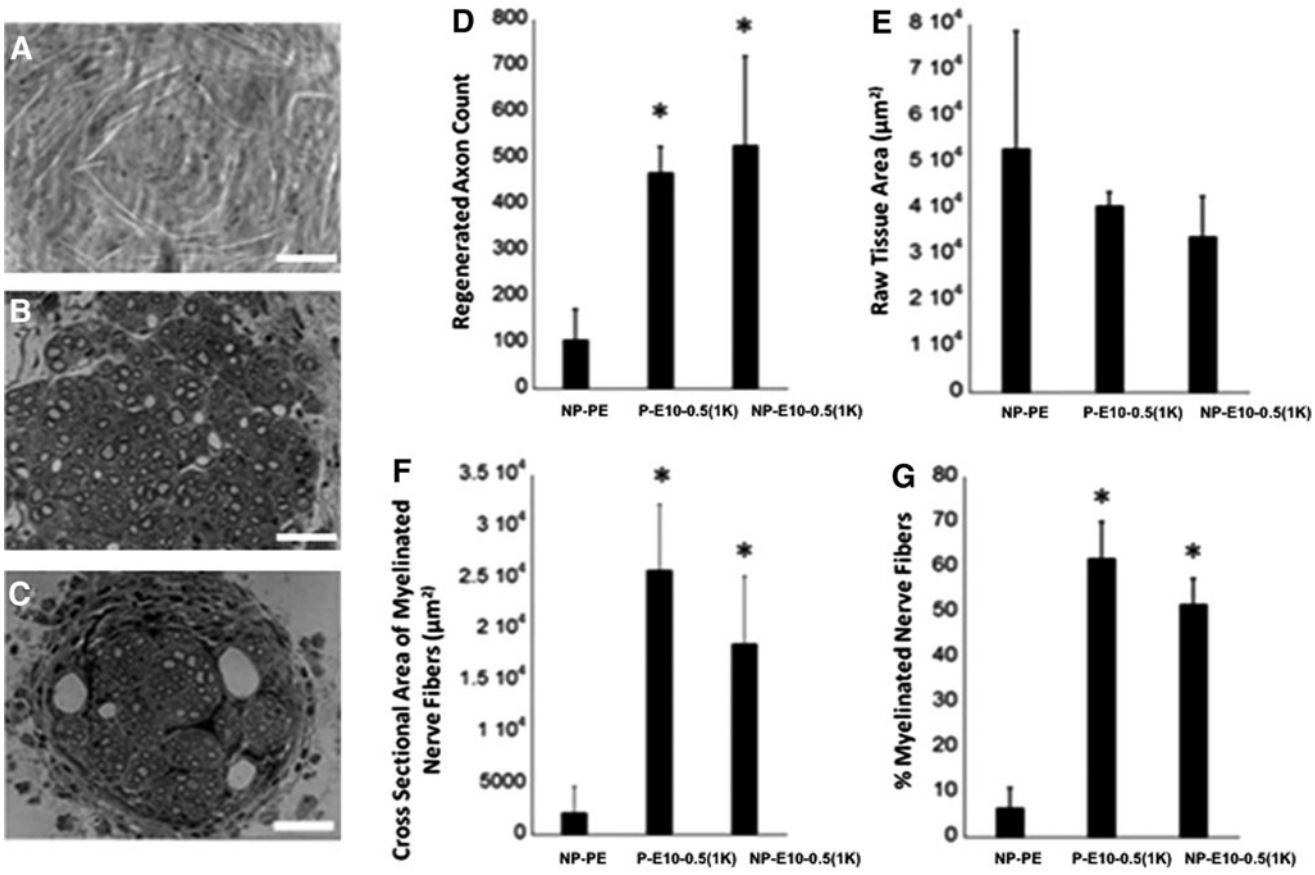

FIG. 6. Histomorphometric analysis of femoral nerves regenerated in E10-0.5(1K) and NP-PE conduits. **(A–C)** Representative cross-sectional images (40×, Scale bar: 50 μm) of nerve sections stained with toluidine blue from the midpoint of regenerated femoral nerve after tubulization with either **(A)** nonporous PE conduits (NP-PE), **(B)** porous E10-0.5(1K) conduits [P-E10-0.5(1K)], or **(C)** nonporous E10-0.5(1K) conduits [NP-E10-0.5(1K)]. **(D)** Axon count of myelinated axons in the regeneration cable in the mid-conduit nerve section for each conduit type. **(E)** Raw tissue area. **(F)** Cross-sectional area of regenerated nerve fibers. **(G)**% myelinated nerve fibers in regenerating nerve cable. *Significant difference between group mean values from NP-PE ($p < 0.05$, one-way analysis of variance with Tukey's *post hoc* test).

In vivo *evaluation*

Motor function recovery. Functional recovery was quantified by SFMA of the FBA and PLR (Fig. 5 A–D), using well-established methods.[40] By week 8, animals that received E10-0.5(1K) conduits showed a marked improvement in the FBA as compared to mice that received NP-PE conduits (Fig. 5E). Improvement of motor function in E10-0.5(1K)-treated animals was also demonstrated by the PLR, irrespective of whether porous or nonporous conduits were used, by as early as 2 weeks (Fig. 5G). Results collected up to 15 weeks demonstrate that the PLR value for animals with E10-0.5(1K) conduits approached pre-surgical values at a faster rate than animals treated with NP-PE.

Calculation of the RI further supported that recovery promoted by E10-0.5(1K) was enhanced over that promoted with PE conduits. Animals that received E10-0.5(1K) conduits achieved RI values approaching 50% for the FBA (Fig. 5F) and 100% for the PLR (Fig. 5H). Animals that received NP-PE conduits demonstrated an average RI value for the FBA of −26% and an average RI value of 23% for the PLR. The tight grouping of the animals within each E10-0.5(1K) group indicates consistent performance in contrast with the variation in the RI values calculated from animals receiving NP-PE conduits. Overall, the functional results indicate that the use of an E10-0.5(1K) conduit results in significant recovery of functional movement, irrespective of E10-0.5(1K) conduit porosity.

Histomorphometric analysis. At the endpoint of the study, nerves were analyzed for histomorphometric features (Fig. 6). A significantly greater number of axons were present within regenerating nerve cables formed within E10-0.5(1K) conduits with a smaller area of raw fibrous tissue, regardless of the presence of pores in the outer walls. The cross-sectional area of the myelinated nerve fibers was significantly greater in all E10-0.5(1K) conduits as compared to the NP-PE conduit, and a greater percentage of this area was occupied by myelinated nerve fibers.

Representative 100× images of 1-μm-thick cross sections postfixed in osmium tetroxide as well as the fiber diameter distribution from each condition are shown in Figure 7. The E10-0.5(1K) conduits generated nerve cables with a large number of axons, fascicular structures, a large range of nerve fiber diameters, and little fibrous tissue, while the NP-PE conduits contained few, if any, evident axons. The inner

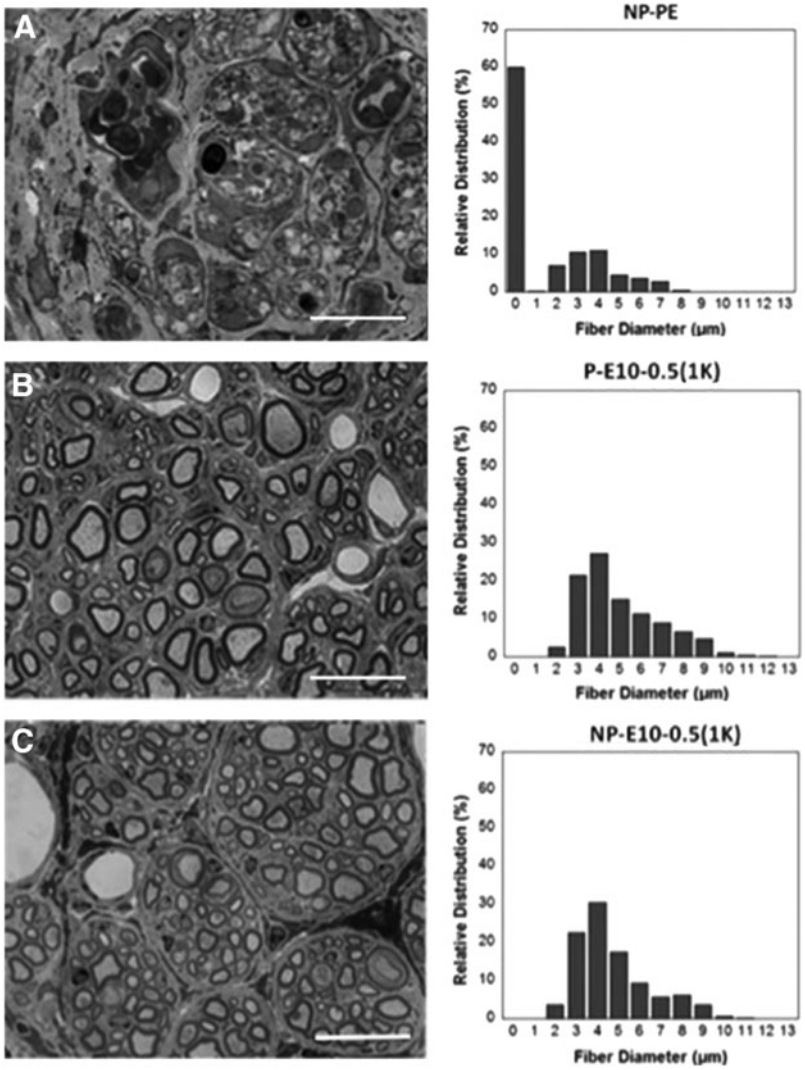

FIG. 7. Representative nerve sections and fiber diameter analysis. Representative cross-sectional images (100×, Scale: 20 μm) of nerve sections stained with toluidine blue from the midpoint of regenerated femoral nerve and histogram of the relative distribution of nerve fiber diameter after tubulization with either **(A)** nonporous PE conduits (NP-PE), **(B)** porous E10-0.5(1K) conduits [P-E10-0.5(1K)], or **(C)** nonporous E10-0.5(1K) conduits [NP-E10-0.5(1K)]. Histograms of fiber diameters reveal a reduced number of small axons and an increased number of larger axons in animals treated with E10-0.5(1K) conduits as compared to animals treated with NP-PE conduits. There was a statistically higher relative distribution (%) of fiber diameters measuring 4, 5, 6, 7, and 8 μm in P-E10-0.5(1K) and NP-E10-0.5(1K) conduits as compared to NP-PE conduits. ($p < 0.05$, one-way analysis of variance with Tukey's *post hoc* test).

lumina were completely filled with what appeared to be dense, fibrous tissue.

Early differences in nerve repair between conduit materials. The initial formation of a fibrin cable helps support axonal in-growth and Schwann cell infiltration and is crucial for determining at an early time point the final outcome of the regenerating nerve cable.[52] We found that longitudinal fibrin strands could be observed 2 weeks post-implantation in E10-0.5(1K) conduits (as indicated by the black arrow in Fig. 8A), but not in NP-PE conduits (Fig. 8A, B), suggesting the initiation of the formation of a fibrin cable across the nerve gap.[53] Furthermore, western blot analysis of Schwann cell markers within nerve exudates 1 week post-implantation revealed a greater abundance of S100ß and GFAP immunoreactivities in exudates removed from E10-0.5(1K) conduits as compared to exudates removed from within NP-PE conduits (Fig. 8C, D).

Discussion

Through this study, we have found that conduit material can play a key role in the regenerative potential of a nerve guidance conduit by directly affecting the key processes associated with successful regeneration, such as protein adsorption, fibrin matrix formation, and Schwann cell infiltration. Conduits fabricated from E10-0.5(1K) outperformed conduits fabricated from PE. Our study also suggests that the conduit material, rather than the wall structure (porosity), can primarily influence the regenerative potential of a conduit *in vivo.* It will be essential to test these conduits for their ability to promote regeneration in larger animal models and in larger, more commonly used nerves, such as the rodent sciatic nerve. Using larger animal models and nerves will make it possible to compare against FDA-approved conduits that are clinically used.

The differences observed between the E10-0.5(1K) and PE conduits in this study may be due to a specific interaction of the regenerating elements, including ECM proteins, Schwann cells, and fibroblasts, with the material constituting the outer conduit wall as numerous studies have shown the role each of these elements has on *in vivo* nerve regeneration.[54–57] Given that histology showed all axons growing in the middle of conduit, it is doubtful that regenerating axons extensively interacted directly with the inner wall of the conduit. Protein adsorption to biomaterials is known to play a significant role in the final regenerative outcome of a nerve conduit, as it is one of initial events post-implantation, and influences later biological events, such as cell attachment and

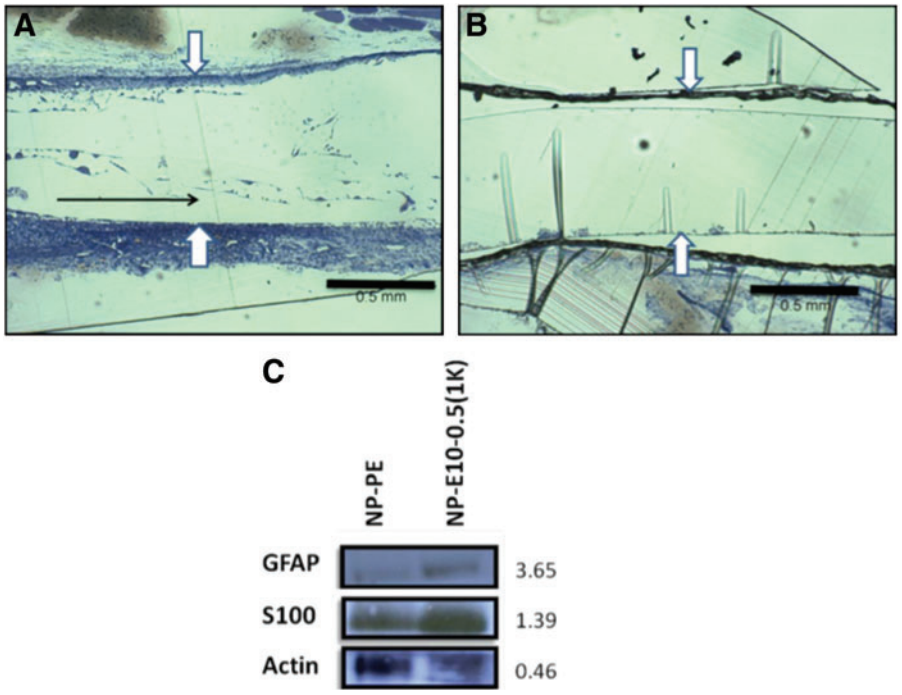

FIG. 8. Early differences in nerve repair between conduit materials. **(A)** and **(B)** show representative images of longitudinal sections of the acellular fibrin matrix within conduits at 2 weeks after implantation. **(A)** The natural matrix found in E10-0.5(1K) conduits. **(B)** The matrix present in NP-PE conduits. The polymers comprising the natural fibrin matrix in the E10-0.5(1K) had a predominant longitudinal orientation **(**black arrow in **A),** whereas no fibrin strands were observed in NP-PE conduits. White arrows mark edges of the inner lumen within each conduit type. Scale bar: 0.5 mm. **(C)** Representative western blot analysis of S100β and glial fibrillary acidic protein (GFAP) collected from nonporous E10-0.5(1K) and NP-PE conduit exudates 1 week after implantation. Values to the right of bands indicate relative optical densities of bands (NP-E10-0.5(1K)/NP-PE). Color images available online at www.liebertpub.com/tea

outgrowth, which occur through a necessary layer of adsorbed proteins.[58] In fact, many new biomaterials are modified to promote protein adsorption, such as grafting with bioactive peptides to encourage cell attachment and migration.[59,60] Post-fabrication, several methods have been employed to determine the capability of the material to adsorb serum proteins *in vitro.* For example, Woo *et al.* investigated the adsorption of fibronectin, laminin, vitronectin, and bovine serum albumin to nanofibrous poly(L-lactic acid) scaffolds using a MicroBCA protein assay kit and found differing amounts of adsorption based on the architecture of the scaffold.[50] Similarly, Wang *et al.* and Cai *et al.* studied protein adsorption from the cell culture medium onto poly(propylene fumarate), poly(caprolactone fumarate), and poly(e-caprolactone acrylate) disks varying within a range of chemical compositions. Findings showed amounts of protein adsorption correlated to sequential changes in the chemical composition of the polymer.[54,61] In this study, E10-0.5(1K) appears to intrinsically encourage protein adsorption. Taken together with data in the literature, it is most likely that conduits fabricated from E10-0.5(1K) stimulated greater adsorption of serum proteins within the inner lumen *in vivo*, consequently enhancing neurite extension and the rate and quality of nerve regeneration.[4,62–65]

Our results also demonstrated that Schwann cell migration into the injury site and fibrin matrix formation are positively influenced by the E10-0.5(1K) composition. Additionally, *in vitro* results showed that Schwann cell attachment and extension on E10-0.5(1K) was significantly greater than on PE. Within the first hours following nerve transection and conduit implantation, wound fluid rich in nerve-supporting factors fills from both nerve stumps into the conduit inner lumen.[65–67] During this process, the fibrin matrix (derived from plasma precursors) accumulates naturally to form a complete bridge across the chamber gap providing a substrate for cellular migration.[51] The E10-0.5(1K) conduit may encourage the early orientation of regenerating components on its own, as opposed to filling the inner lumen with a synthetic material to act as a longitudinal cable.[68–70] This may occur by increasing infiltrating Schwann cells and fibroblasts across the nerve injury gap accelerating the temporal progress of regeneration.

Longitudinal sections (Fig. 8 and additional samples not shown) demonstrate that the fibrin matrix develops within the E10-0.5(1K) conduits earlier than within the NP-PE conduits. This matrix behaves as a physical scaffold for non-neuronal calls, including fibroblasts, Schwann cells, macrophages, and endothelial cells to influence axonal elongation and initiate the regenerative process.[51,71] Due to the critical role Schwann cells play in nerve regeneration, we used biochemical analysis techniques (Fig. 8C) to investigate the presence of proteins specific to Schwann cells within the nerve conduits post-implantation.[51,57,64,72,73] Results showed that these protein levels were higher in E10-0.5(1K) conduits as compared to conduits fabricated from PE. Although equal total amounts of protein were analyzed, western blot analyses show that standard proteins, GAPDH and ß-actin, both intracellular, were higher in the PE as compared to the E10-0.5(1K) material. This finding indicates that relatively more intracellular proteins were present within the NP-PE conduits than within the E10-0.5(1K) conduits, and conversely, more extracellular proteins were present within the E10-0.5(1K) conduits than within the NP-PE conduits.

In addition to material compositions playing a key role in the regenerative potential of a conduit, we investigated whether or not the presence of pores in the outer conduit wall plays a role. Some reports demonstrate benefits of using porous nerve conduits, which are hypothesized to facilitate the flow of nutrients and factors that enhances cell migration and fibrin cable formation,[74,75] while others show the benefits of using nonporous conduits, which better contain the fluid and cells secreted by the nerve stumps at the injury site,

in direct association with the regenerating axons.[76] However, very few studies directly compare porous to nonporous nerve conduits. Of the small number of studies that do compare the two, no study directly compares a single layer nonporous and porous conduit fabricated from the same material as we did in this study using E10-0.5(1K). Our results show no statistical differences between the functional recovery of the animals treated with a P-E10-0.5(1K) conduit or a NP-E10-0.5(1K) conduit or in the quality of the nerve regenerated, implying that both conduits have similar effects on the nerve regeneration outcome. It is possible that the improved interactions with exudate proteins outweigh the benefits of having pores within the outer conduit walls. In longer nerve gaps, or in the treatment of larger diameter nerves, the presence of pores in the outer conduit wall may have an additional beneficial effect not seen in this study. Additionally, for materials that are not as apparently beneficial as E10-0.5(1K) on nerve regeneration, porosity may be more of a driving factor in successful regeneration, allowing for greater diffusion of nutrients, growth factors, and cells into the inner lumen and may help to develop and sustain a viable fibrin matrix across the entire length of the nerve gap.[77]

When E10-0.5(1K) conduits were compared against a NP-PE conduit, animals treated with E10-0.5(1K) conduits statistically performed better. Transection of the femoral nerve leads to atrophy of the quadriceps muscle and prevents proper extension, which can be visualized during individual steps of the mouse taken during the normal walking cycle.[40] Functional results for the FBA test as early as week 6 post-injury clearly illustrate that functional recovery is sensitive to the type of conduit used, and that an E10-0.5(1K) conduit improves function as compared to a NP-PE conduit. The FBA for animals treated with NP-PE conduits remained constant at an elevated value of $\sim 100°$ throughout the 15-week study. This finding is in accordance with other studies in which NP-PE conduits filled with saline were used to repair a 5 mm transection in the mouse femoral nerve.[41] Additionally, results from the PLR, which evaluate the ability of the mouse to voluntarily extend the knee joint without any body weight support, demonstrate that animals treated with E10-0.5(1K) conduits performed significantly better than animals treated with NP-PE conduits.

Conclusions

The present study provides significant new observations on the interplay between the material properties of a nerve conduit and the axonal response observed both *in vitro* and *in vivo*. In this study, we used a specific polymer composition [E10-0.5(1K)] selected from a combinatorially designed polymer library of over 10,000 distinct tyrosine-derived polycarbonate compositions. Whereas E10-0.5(1K) clearly outperformed a conventional PE conduit, it is possible that the tyrosine-derived polycarbonate library contains polymer compositions that may perform even better. Our results indicate that one potential way to discover these compositions is to screen polymer candidates for their ability to absorb neuroinductive ECM molecules on their surface. A second observation is related to the side-by-side comparison of porous and nonporous E10-0.5(1K) conduits in a critical size defect in the mouse femoral nerve. Based on the data presented here, we conclude that in this particular animal model, conduit porosity is not affecting nerve regeneration. We recognize that additional comparisons of porous and nonporous conduits in different animal models are needed, before we can reach a final conclusion on the long-debated question of the advantages of porous nerve regeneration conduits.

Acknowledgments

This research was sponsored by the Armed Forces Institute of Regenerative Medicine award number W81XWH-08-2-0034. The US Army Medical Research Acquisition Activity, 820 Chandler Street, Fort Detrick MD 21702-5014 is the awarding and administering acquisition office. The content of the manuscript does not necessarily reflect the position or the policy of the Government, and no official endorsement should be inferred. Research was conducted in compliance with the Animal Welfare Act Regulations and other Federal statutes relating to animals and experiments involving animals and adheres to the principles set forth in the Guide for Care and Use of Laboratory Animals, National Research Council, 1996. This work was also supported by the Center for Military Biomaterials Research (CeMBR) award number W81XWH-04-2-0031 and the New Jersey Center for Biomaterials at Rutgers University. The authors would like to thank Dr. Jian Chen for performing the surgeries, Dr. Ijaz Ahmed for preparation of the tissue samples, and Anna Yang for helping with the Schwann cell experiments.

Disclosure Statement

No competing financial interests exist.

References

1. Noble, J., Munro, C.A., Prasad, V.S.S.V., and Midha, R. Analysis of Upper and Lower Extremity Peripheral Nerve Injuries in a Population of Patients with Multiple Injuries. Baltimore, MD: Lippincott Williams & Wilkins, 1998.
2. Schlosshauer, B., Dreesmann, L., Schaller, H.-E., and Sinis, N. Synthetic nerve guide implants in humans: a comprehensive survey. Neurosurgery **59,** 740, 2006.
3. Gordon, T., Chan, K.M., Sulaiman, O.A.R., Udina, E., Amirjani, N., and Brushart, T.M. Accelerating axon growth to overcome limitations in functional recovery after peripheral nerve injury. Neurosurgery **65,** A132, 2009.
4. Belkas, J.S., Shoichet, M.S., and Midha, R. Peripheral nerve regeneration through guidance tubes. Neurol Res **26,** 151, 2004.
5. Kemp, S.W.P., Walsh, S.K., and Midha, R. Growth factor and stem cell enhanced conduits in peripheral nerve regeneration and repair. Neurol Res **30,** 1030, 2008.
6. Kleene, R., and Schachner, M. Glycans and neural cell interactions. Nat Rev Neuroscience **5,** 195, 2004.
7. Bellamkonda, R.V. Peripheral nerve regeneration: an opinion on channels, scaffolds and anisotropy. Biomaterials **27,** 3515, 2006.
8. Madison, R., Archibald, S., and Krarup, C. Peripheral wound injury. In: Cohen, I., Diegemann, R., Lindblad, W., eds. Wound Healing: Biochemical and Clinical Aspects. Philadelphia, PA: W.B. Saunders, 1992. pp. 450–487.
9. Stang, F., Keilhoff, G., and Fansa, H. Biocompatibility of different nerve tubes. Materials **2,** 1480, 2009.
10. Heijke, G.C.M., Klopper, P.J., Van Doorn, I.B.M., and Baljet, B. Processed porcine collagen tubulization versus conventional suturing in peripheral nerve reconstruction: an experimental study in rabbits. Microsurgery **21,** 84, 2001.

11. Jiang, X., Lim, S.H., Mao, H.-Q., and Chew, S.Y. Current applications and future perspectives of artificial nerve conduits. Exp Neurol **223,** 86, 2010.
12. Inada, Y., Morimoto, S., Moroi, K., Endo, K., and Nakamura, T. Surgical relief of causalgia with an artificial nerve guide tube: successful surgical treatment of causalgia (Complex Regional Pain Syndrome Type II) by *in situ* tissue engineering with a polyglycolic acid-collagen tube. Pain **117,** 251, 2005.
13. Braga-Silva, J. The use of silicone tubing in the late repair of the median and ulnar nerves in the forearm. J Hand Surg [Br] **24,** 703, 1999.
14. Seckel, B.R., Jones, D., Hekimian, K.J., Wang, K.K., Chakalis, D.P., and Costas, P.D. Hyaluronic acid through a new injectable nerve guide delivery system enhances peripheral nerve regeneration in the rat. J Neurosci Res **40,** 318, 1995.
15. Mehanna, A., Mishra, B., Kurschat, N., Schulze, C., Bian, S., Loers, G., *et al.* Polysialic acid glycomimetics promote myelination and functional recovery after peripheral nerve injury in mice. Brain **132,** 1449, 2009.
16. Inoe, A.P., Pereira, F.C., Stopiglia, A.J., and Da-Silva, C.F. Pharmacological immunomodulation enhances peripheral nerve regeneration. Pesq Vet Bras **27,** 363, 2007.
17. Bryan, D.J., Wang, K.-K., and Chakalis-Haley, D.P. Effect of Schwann cells in the enhancement of peripheral-nerve regeneration. J Reconstr Microsurg **12,** 439, 1996.
18. Panseri, S., Cunha, C., Lowery, J., Del Carro, U., Taraballi, F., Amadio, S., *et al.* Electrospun micro- and nanofiber tubes for functional nervous regeneration in sciatic nerve transections. BMC Biotechnol **8,** 39, 2008.
19. Bryan, D.J., Holway, A.H., Wang, K.K., Silva, A.E., Trantolo, D.J., Wise, D., *et al.* Influence of glial growth factor and Schwann cells in a bioresorbable guidance channel on peripheral nerve regeneration. Tissue Eng **6,** 129, 2000.
20. Meek, M.F., and Coert, J.H. US Food and Drug Administration/Conformit Europe-approved absorbable nerve conduits for clinical repair of peripheral and cranial nerves. Ann Plast Surg **60,** 466, 2008.
21. Yannas, I.V., and Hill, B.J. Selection of biomaterials for peripheral nerve regeneration using data from the nerve chamber model. Biomaterials **25,** 1593, 2004.
22. Kokai, L.E., Bourbeau, D., Weber, D., McAtee, J., and Marra, K.G. Sustained growth factor delivery promotes axonal regeneration in long gap peripheral nerve repair. Tissue Eng Part A **17,** 1263, 2011.
23. Nectow, A.R., Marra, K.G., and Kaplan, D.L. Biomaterials for the development of peripheral nerve guidance conduits. Tissue Eng Part B Rev **18,** 40, 2012.
24. Sundback, C., Hadlock, T., Cheney, M., and Vacanti, J. Manufacture of porous polymer nerve conduits by a novel low-pressure injection molding process. Biomaterials **24,** 819, 2003.
25. Zhu, Y., Wang, A., Patel, S., Kurpinski, K., Diao, E., Bao, X., *et al.* Engineering bi-layer nanofibrous conduits for peripheral nerve regeneration. Tissue Eng Part C Methods **17,** 705, 2011.
26. Brunelli, G.A., Vigasio, A., and Brunelli, G.R. Invited review: Different conduits in peripheral nerve surgery. Microsurgery **15,** 176, 1994.
27. Strauch, B. Use of nerve conduits in peripheral nerve repair. Hand Clin **16,** 123, 2000.
28. Kehoe, S., Zhang, X.F., and Boyd, D. FDA approved guidance conduits and wraps for peripheral nerve injury: a review of materials and efficacy. Injury **43,** 553, 2012.
29. Meek, M.F., and Coert, J.H. Clinical use of nerve conduits in peripheral-nerve repair: review of the literature. J Reconstr Microsurg **18,** 97, 2002.
30. Meek, M.F., and Coert, J.H. US Food and Drug Administration/Conformit Europe-approved absorbable nerve conduits for clinical repair of peripheral and cranial nerves. Ann Plast Surgery **60,** 466, 2008.
31. Zeltinger, J., Schmid, E., Brandom, D., Bolikal, D., Pesnell, A., and Kohn, J. Advances in the development of coronary stents. Biomater Forum **26,** 8, 2004.
32. Choueka, J., Charvet, J.L., Koval, K.J., Alexander, H., James, K.S., Hooper, K.A., *et al.* Canine bone response to tyrosine-derived polycarbonates and poly(L-lactic acid). J Biomed Mater Res **31,** 35, 1996.
33. Abramson, S.D. Selected bulk and surface properties and biocompatibility of a new class of tyrosine-derived polycarbonates. New Brunswick: Rutgers Univeristy and University of Medicine and Dentistry of New Jersey and Robert Wood Johnson Medical School, 2002.
34. Brocchini, S., James, K., Tangpasuthadol, V., and Kohn, J. Structure–property correlations in a combinatorial library of degradable biomaterials. J Biomed Mater Res **42,** 66, 1998.
35. Hooper, K.A., Macon, N.D., and Kohn, J. Comparative histological evaluation of new tyrosine-derived polymers and poly (L-lactic acid) as a function of polymer degradation. J Biomed Mater Res **41,** 443, 1998.
36. Brushart, T. Motor axons preferentially reinnervate motor pathways. J Neurosci **13,** 2730, 1993.
37. Brushart, T. Preferential reinnervation of motor nerves by regenerating motor axons. J Neurosci **8,** 1026, 1988.
38. Brushart, T.M.E., and Seiler Iv, W.A. Selective reinnervation of distal motor stumps by peripheral motor axons. Exp Neurol **97,** 289, 1987.
39. Ahlborn, P., Schachner, M., and Irintchev, A. One hour electrical stimulation accelerates functional recovery after femoral nerve repair. Exp Neurol **208,** 137, 2007.
40. Irintchev, A., Simova, O., Eberhardt, K.A., Morellini, F., and Schachner, M. Impacts of lesion severity and tyrosine kinase receptor B deficiency on functional outcome of femoral nerve injury assessed by a novel single-frame motion analysis in mice. Eur J Neurosci **22,** 802, 2005.
41. Masand, S.N., Chen, J., Perron, I.J., Hammerling, B.C., Loers, G., Schachner, M., *et al.* The effect of glycomimetic functionalized collagen on peripheral nerve repair. Biomaterials **33,** 8353, 2012.
42. Irintchev, A. Potentials and limitations of peripheral nerve injury models in rodents with particular reference to the femoral nerve. Ann Anat **193,** 276, 2011.
43. Simova, O., Irintchev, A., Mehanna, A., Liu, J., Dihné, M., Bächle, D., *et al.* Carbohydrate mimics promote functional recovery after peripheral nerve repair. Ann Neurol **60,** 430, 2006.
44. Yannas, I., and Zhang, M. Regeneration of a peripheral nerve. Tissue and Organ Regeneration in Adults. Chernow Editorial Services managed by Francine McNeill, New York: Springer, 2001, pp. 138–185.
45. Gomez, N., Cuadras, J., Buti, M., and Navarro, X. Histologic assessment of sciatic nerve regeneration following resection and graft or tube repair in the mouse. Restor Neurol Neurosci **10,** 187, 1996.
46. Magno, M.H.R., Kim, J., Srinivasan, A., McBride, S., Bolikal, D., Darr, A., *et al.* Synthesis, degradation and biocompatibility of tyrosine-derived polycarbonate scaffolds. J Mater Chem **20,** 8885, 2010.
47. Honkanen, H., Lahti, O., Nissinen, M., Myllylä, R.M., Kangas, S., Päiväläinen, S., *et al.* Isolation, purification and expansion of myelination-competent, neonatal mouse Schwann cells. Eur J Neurosci **26,** 953, 2007.

48. Irintchev, A., Wu, M.-M., Lee, H.J., Zhu, H., Feng, Y.-P., Liu, Y.-S., *et al.* Glycomimetic improves recovery after femoral injury in a non-human primate. J Neurotrauma **28,** 1295, 2011.
49. Kaewkhaw, R., Scutt, A.M., and Haycock, J.W. Anatomical site influences the differentiation of adipose-derived stem cells for Schwann-cell phenotype and function. Glia **59,** 734, 2011.
50. Woo, K.M., Chen, V.J., and Ma, P.X. Nano-fibrous scaffolding architecture selectively enhances protein adsorption contributing to cell attachment. J Biomed Mater Res A **67A,** 531, 2003.
51. Williams, L.R. Exogenous fibrin matrix precursors stimulate the temporal progress of nerve regeneration within a silicone chamber. Neurochem Res **12,** 851, 1987.
52. Clements, I.P., Kim, Y.T., English, A.W., Lu, X., Chung, A., and Bellamkonda, R.V. Thin-film enhanced nerve guidance channels for peripheral nerve repair. Biomaterials **30,** 3834, 2009.
53. Zhao, Q., Dahlin, L.B., Kanje, M., and Lundborg, G. Repair of the transected rat sciatic nerve: matrix formation within implanted silicone tubes. Restor Neurol Neurosci **5,** 197, 1993.
54. Cai, L., and Wang, S. Poly-ε-caprolactone acrylates synthesized using a facile method for fabricating networks to achieve controllable physicochemical properties and tunable cell responses. Polymer **51,** 164, 2010.
55. Wang, L.-P., Wang, W., Di, L., Lu, Y.-N., and Wang, J.-Y. Protein adsorption under electrical stimulation of neural probe coated with polyaniline. Colloids Surf B Biointerfaces **80,** 72, 2010.
56. Wang, S., and Cai, L. Polymers for fabricating nerve conduits. Int J Polym Sci **2010,** Article ID 138686, 2010.
57. Armstrong, S.J., Wiberg, M., Terenghi, G., and Kingham, P.J. ECM molecules mediate both Schwann cell proliferation and activation to enhance neurite outgrowth. Tissue Eng **13,** 2863, 2007.
58. Soria, J.M., Martínez Ramos, C., Bahamonde, O., García Cruz, D.M., Salmerón Sánchez, M., García Esparza, M.A., *et al.* Influence of the substrate's hydrophilicity on the *in vitro* Schwann cells viability. J Biomed Mater Res A **83A,** 463, 2007.
59. Rafiuddin Ahmed, M., and Jayakumar, R. Peripheral nerve regeneration in RGD peptide incorporated collagen tubes. Brain Res **993,** 208, 2003.
60. Yu, T.T., and Shoichet, M.S. Guided cell adhesion and outgrowth in peptide-modified channels for neural tissue engineering. Biomaterials **26,** 1507, 2005.
61. Wang, S., Kempen, D.H., Simha, N.K., Lewis, J.L., Windebank, A.J., Yaszemski, M.J., *et al.* Photo-cross-linked hybrid polymer networks consisting of poly(propylene fumarate) and poly(caprolactone fumarate): controlled physical properties and regulated bone and nerve cell responses. Biomacromolecules **9,** 1229, 2008.
62. Kotwal, A., and Schmidt, C.E. Electrical stimulation alters protein adsorption and nerve cell interactions with electrically conducting biomaterials. Biomaterials **22,** 1055, 2001.
63. Schmidt, C.E., Shastri, V.R., Vacanti, J.P., and Langer, R. Stimulation of neurite outgrowth using an electrically conducting polymer. Proc Natl Acad Sci U S A **94,** 8948, 1997.
64. Dalton, P.D., and Mey, J. Neural Interactions with materials. Frontiers in Bioscience **1,** 769, 2009.
65. Longo, F.M., Hayman, E.G., Davis, G.E., Ruoslahti, E., Engvall, E., Manthorpe, M., *et al.* Neurite-promoting factors and extracellular matrix components accumulating *in vivo* within nerve regeneration chambers. Brain Res **309,** 105, 1984.
66. Liu, H.M. The role of extracellular matrix in peripheral nerve regeneration: a wound chamber study. Acta Neuropathol **83,** 469, 1992.
67. Weis, J., May, R., and Schröder, J. Fine structural and immunohistochemical identification of perineurial cells connecting proximal and distal stumps of transected peripheral nerves at early stages of regeneration in silicone tubes. Acta Neuropathol **88,** 159, 1994.
68. Cai, J., Peng, X.J., Nelson, K.D., Eberhart, R., and Smith, G.M. Permeable guidance channels containing microfilament scaffolds enhance axon growth and maturation. J Biomed Mater Res A **75A,** 374, 2005.
69. Hu, W., Gu, J.H., Deng, A.D., and Gu, X.S. Polyglycolic acid filaments guide Schwann cell migration *in vitro* and *in vivo*. Biotechnol Lett **30,** 1937, 2008.
70. Kim, Y.T., Haftel, V.K., Kumar, S., and Bellamkonda, R.V. The role of aligned polymer fiber-based constructs in the bridging of long peripheral nerve gaps. Biomaterials **29,** 3117, 2008.
71. Williams, L.R., Longo, F.M., Powell, H.C., Lundborg, G., and Varon, S. Spatial-Temporal progress of peripheral nerve regeneration within a silicone chamber: Parameters for a bioassay. J Comp Neurol **218,** 460, 1983.
72. Wang, G.-Y., Hirai, K.-I., and Shimada, H. The role of laminin, a component of Schwann cell basal lamina, in rat sciatic nerve regeneration within antiserum-treated nerve grafts. Brain Res **570,** 116, 1992.
73. Cornbrooks, C.J., Carey, D.J., McDonald, J.A., Timpl, R., and Bunge, R.P. *In vivo* and *in vitro* observations on laminin production by Schwann cells. Proc Natl Acad Sci U S A **80,** 3850, 1983.
74. Jenq, C.-B., and Coggeshall, R.E. Permeable tubes increase the length of the gap that regenerating axons can span. Brain Res **408,** 239, 1987.
75. Vleggeert-Lankamp, C.L.A.M., de Ruiter, G.C., Wolfs, J.F.C., Pêgo, A.P., van den Berg, R.J., Feirabend, H.K.P., *et al.* Pores in synthetic nerve conduits are beneficial to regeneration. J Biomed Mater Res A **80A,** 965, 2007.
76. Meek, M.F., and Dunnen, W.F.A.D. Porosity of the wall of a Neurolac® nerve conduit hampers nerve regeneration. Microsurgery **29,** 473, 2009.
77. Kokai, L.E., Lin, Y.-C., Oyster, N.M., and Marra, K.G. Diffusion of soluble factors through degradable polymer nerve guides: Controlling manufacturing parameters. Acta Biomater **5,** 2540, 2009.

Address correspondence to:
Melitta Schachner, PhD
W.M. Keck Center for Collaborative Neuroscience
Rutgers, The State University of New Jersey
604 Allison Road, D-251
Piscataway, NJ 08854

E-mail: Schachner@biology.rutgers.edu

Joachim Kohn, PhD
New Jersey Center for Biomaterials
Rutgers, The State University of New Jersey
145 Bevier Road
Piscataway, NJ 08854

E-mail: kohn@rutgers.edu

Received: February 7, 2013
Accepted: September 3, 2013
Online Publication Date: November 11, 2013